



Design of a Mini Double-Discharge Centrifugal Pump under Multiphase Flow by CFD and Experimental Verification

Z. Parlak^{1†}, M. Kemerli¹, T. Engin¹ and Y. Koç²

¹ Department of Mechanical Engineering, Sakarya University, Serdivan, Sakarya, 54187, Turkey

² Arçelik A.Ş. Tuzla, İstanbul, 34950, Turkey

†Corresponding Author Email: zparlak@sakarya.edu.tr

(Received March 15, 2018; accepted May 14, 2018)

ABSTRACT

Pumps are irreplaceable products in various systems and processes. Pumps can be manufactured in various size in industry. The mini pumps are commonly used in some household electrical appliances, automobile etc. Some pumping applications is required two outlet ports. The use of two pumps in such a case brings high costs. Instead, pumping on two different lines with a single pump provides both a more compact design and lower cost, if the system is available. In this study, it is aimed to design a single-suction and double-outlet pump by using a single electric motor. For this purpose, a conceptual design for the pump has been proposed and design parameters which have an effect on the pump performance have been determined. Pump performance have been calculated by using the ANSYS Fluent, Computational Fluid Dynamics (CFD) code considering to multiphase flow, and optimization studies have been performed with the determined parameters. The pumps have been obtained by the optimization works have been manufactured and tested to investigate whether the pumps provide the expected operating conditions and performances. Finally, the CFD results have been verified by the tests and the pump provided the expected operating conditions and performances.

Keywords: Pump design; Centrifugal pump; Double-outlet pump; CFD; Multiphase flow.

NOMENCLATURE

b	width of the impeller	α	volume of fraction
C	model constant	ε	dissipation rate
F	force	η	efficiency
g	acceleration of gravity	μ	viscosity
G_k	production of turbulence kinetic energy	ρ	density
H	head	σ	model constant
k	turbulence kinetic energy	ϕ	flow coefficient
\dot{m}	mass flow rate	ψ	head coefficient
P	pressure		
Q	flow rate	subscript	
r	tip diameter	d	discharge
S	mass source	m	mixture
t	time	q,p	phase of fluid
V	velocity	s	suction
\dot{W}	power	t	turbulence
z	distance		

1. INTRODUCTION

Centrifugal pump is one of the most commonly used hydraulic machines in the world which is used for pressurizing and transferring fluids. These

pumps have various application fields from a micropump to a giant industrial pump. It consists of two main parts called diffuser and impeller that energizes the fluid. Small-scale centrifugal pumps are also used with many systems and their design is

also important.

Many works has been done on the general design and performance aspects of a centrifugal pump. The impeller usually consists of several different blades with a certain curvature. These blades are located around the impeller with equal angles. With the rotation of the impeller, the fluid is sucked from the eye and tangentially discarded by centrifugal movement (Munson *et al.* 2012). While the static pressure and the velocity are increased along the impeller, diffuser converts the kinetic energy to pressure energy of the fluid leaving the impeller (Dixon and Hall 2010). Flow rate against a given head at a given efficiency while a pump can discharge provides a measurement of pump performance (Cooper *et al.* 2008).

The pump efficiency which depends on design parameters of impeller and diffuser of a pump is needed to increase the pump performance. Accordingly, researchers focus on improving pump performance by optimizing the design parameters. Most of the optimization methods of centrifugal pumps are high cost and time-consuming (Zhang *et al.* 2014). Jafarzadeh *et al.* (2011) discussed the effects of different blade numbers and blade positions on results of the continuous regime and revealed the effects of these parameters on the solving. Zhou *et al.* (2003) studied the relationship between different blade types and the efficiency. They have come to the conclusion that folded blade structures are more efficient. Olszewski (2016) has pointed to the topic of energy efficiency and optimization of multi-pumping systems in his study. Since centrifugal pumps consume a huge energy from energy resources of each nation. It is necessary to improve the efficiency of pumps by optimization methods.

Computational Fluid Dynamics (CFD) Methods have recently been used to develop designs of the pumps and to provide data about their internal flows. There are different techniques to model a centrifugal pump by CFD. The Mixing Plane, Moving Reference Frame (MRF) and Sliding Mesh methods can be considered the prominent techniques (Shah *et al.* 2013, Petit *et al.* 2009). The first two methods are used at steady-state analysis while the other is used at transient analysis. The MRF method is more useful for simulation of full pump body (Dick *et al.* 2001, Damor *et al.* 2013, Shah *et al.* 2010).

CFD is also used to find out the purpose of optimization and the effect on performance of design parameters. Singh and Nataraj (2012) have presented a methodology to find optimum centrifugal blower design for performance improvement. The chosen parameters which are impeller width, impeller outlet diameter, the thickness of blade and impeller inlet diameter are combined based on Taguchi orthogonal array to determine the required experimental trials. The experimental results have been compared with CFD results and a fine conformity was found. Ling *et al.* (2011) have carried out a study to optimize the impeller design parameters to improve the

performance of the centrifugal pump. 16 impellers have been modeled according to an orthogonal array based on five impeller geometric parameters and simulated in the same volute by the same numerical methods. The efficiency and the head of the optimal pump have been captured by the variance analysis method in best values of the five parameters have been shown a significant improvement compared with the original pump. The modeling of centrifugal pumps has not yet reached a certain standard in the field of CFD. There are different studies about different methods related to this subject. Miguel Asuaje *et al.* (2005) examined the volute-blade relationship and found that the forces coming to the impeller change with time. Dick *et al.* (2001) compared the results between the experimental results with the Sliding Mesh Method (SMM), the Mixed Plane Method (MPM) and the Multiple Reference Fields (MRF) methods for the centrifugal pump. They have concluded that non-transient solutions have a risk of deviating from actual results. The transient characteristics of a centrifugal pump during the starting period have investigated by Chalghoum *et al.* (2016). The comparison between the numerical and experimental results of the pump characteristic curve has shown a good concordance. Barrio *et al.* (2010) examined the irregularities of the output geometry in different flow rates in their study for irregular regions in the pump geometry. Grapsas *et al.* (2008) have performed a CFD analysis of the incompressible turbulent flow through in the test impeller and found an agreement with the corresponding measurements of the impeller of a pump in a laboratory. Also, they have examined the influence of some blade design parameters, like the blade length, the inlet height, and the leading edge inclination, on the performance and the efficiency of the impeller. Spence and Amaral-Teixeira (2009) have used a CFD code to investigate the pressure pulsations for a double entry and volute centrifugal pump. Four geometric parameters which are blade arrangement, cutwater gaps, sidewall clearance and nubber gap have been taken consideration in the investigation. It was revealed that the cutwater gap and blade arrangement have the greatest influence at the monitored locations and the flow range.

Sometimes, some modifications are needed to fulfill a specified task because of such a wide use. One of those modifications is to use the pump with one inlet and two outlets. By using this method, it is possible to transfer the fluid through different passages for different purposes. The first invention goes back to 1950's which can be considered the father of all inventions in this issue, patented in 1959 by Francois (1959). The invention simply proposes a regular centrifugal pump with moving vanes inside to enable the fluid flow through different outlets regarding of the rotation of the impeller. From that time up until now, there are various inventions propose different double outlet centrifugal pumps with different valve elements or diaphragm structures. Most of the inventions have a mechanism which can select the outlet port by changing the rotation of the impeller. These special pumps are widely used for automobile window

washers and various home appliances. Unfortunately, using a diaphragm or a valve brings some problems such as breakage, jamming, fatigue of various elements, loss of flexibility. To overcome such problems the best way is to design a double outlet centrifugal pump without any moving components. Even though the first invention by Douglas (1964) goes back to 1960's in this regard, there is no any improvements exist in the literature. The latest invention is proposed by Park (2012) in 2012 as a patent, which offers two reflectors inside a centrifugal pump body with two outlets which direct the flow through different outlets depending on the rotation of the impeller. The invention is quite similar to the Francois(1959)'s one, except the reflectors are not moving and this makes the pump long lasting. But the geometry of the pump cannot prevent the flow from both outlets at the same time and it is not so appropriate to use this pump for practical purposes.

In this study, it has been intended to design pump which has single-suction and double-outlet. The pump should work manner that when the impeller of the pump rotates one direction fluid is delivered to one outlet line and when rotates the other direction the fluid is delivered to the other outlet. There have been build-in vanes placed in the pump body which prevents the liquid exit from one outlet depending on the direction of the rotation. The pump impeller has been also eccentric from the center of the pump volute. The design process of the centrifugal pumps requires an analytical modeling and tests which takes a lot of time, effort and costs money. But CFD is one of the most promising development in fluid mechanics in the last two decades and gaining more and more attention by the engineers and scientists. By using these numerical methods, it is much easier to design a centrifugal pump without producing a big number of prototypes. In this study, it has been aimed to analyze a double outlet centrifugal pump and trying to understand the physical phenomenon inside and create an optimum design by using CFD. The physical phenomenon inside the pump is a little bit complicated since while the fluid is discharged from one outlet, the other outlet has to be filled with air. Also, as the fluid velocity gets higher, the pressure decreases and this can lead the air to penetrate inside the pump body which may halt the operation of the pump. In contrast, if the flow velocity gets slower, the pressure rises and this might result in the discharge of the fluid from both outlets. This situation is not a desired working condition either. Therefore, the whole hydraulic structure is important and a complete model is needed with a high number of mesh elements. Also, to model the real physics, a multiphase simulation is necessary. Therefore, a steady-state MRF analysis has been preferred to decrease the computational cost.

2. DESIGN AND OPTIMIZATION METHODS

2.1 Geometrical Design

The pump, which is going to be developed in the study, is a single-suction and double-outlet. It is expected that the pump will deliver the liquid to one

of the outlet pipes (discharge line) while the impeller rotates to one direction and deliver to the other outlet pipe (recirculation line) when it rotates to the other direction. Because of this, the impeller was designed as flat, if a curved impeller was designed, one side would be efficient while the other would either be inefficient or could not provide the expected head and head. There is also no need for a curved impeller design because the expected flow rates and pressures are low in the machines used by the pump. While the water rushes to one of the outlet pipes, it is expected that there will be no escape or vacuum at the other pipe. A new concept pump draft is depicted which can be seen Fig. 1. The concept pump is a different volute structure to provide a pressure rise through one of the outlets and prevent the flow from the other outlet. The impeller chamber is located eccentrically and this results in higher velocity values in the vicinity of the upper part of the pump. The expected performance of the pump is 0.0232 flow coefficient in discharge line and 0.0116 flow coefficient in recirculation line.

The four design parameters, the most effective on the pump performance, were selected in the pump body to optimize the pump. A single impeller diameter was used for the fixed pump body diameter. Also the impeller width and the diameters of the outlet pipes of the pump were fixed. As such, number of the parameters was limited. In addition, the number of parameters being able to possible for the design was reduced by re-formulating the relations between the dependent parameters. The four parameters in this study are as follows and the parameters are shown in Fig. 1.

- Expansion Rate
- Upper Gap
- Stopper Length
- Eye Diameter

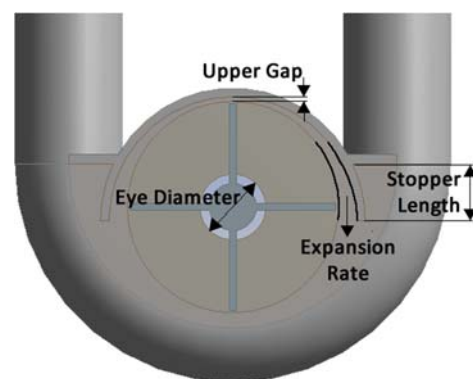


Fig. 1. Geometric parameters on the pump body

- The upper gap is defined as the distance between the top of the impeller and the top of the pump body. This gap is located where the impeller is in its closet position to the pump body. As the impeller gets closer the pump body, the velocity of the fluid increases and the static pressure drops. After passing this narrow gap, as the impeller sweeps the body the

velocity of the fluid becomes decreasing toward to the outlet the static pressure increases.

- The expansion rate is the ratio the upper gap length at the top of the pump to the distance of the impeller tip to the stopper.
- Overflow in the other line through which pump operated is controlled by the stopper length.
- It has been seen in our previous studies that the eye diameter is one of the most effective parameters. The water level or vacuum at the pipe where no fluid is transferred can be controlled by this parameter.

2.2 Mathematical Models

Governing Equations

In the CFD model in this study was designed to model the pump with the whole pipeline geometry. It was aimed to simulate whole physics in order to understand whether the pump realizes the expected performance. By doing so the water level at one outlet can be monitored.

In the CFD model, the desired flow rate which passed through the outlet of the pump and the pressure at the inlet of pump were the determined input values. The pressure at the outlet was calculated depending on these input values. The multiphase model which takes the air and the water into account and k-ε turbulence model were used. It was necessary to use a multiphase model since there is a significant vacuum effect occurs at the one outlet. The initial condition was set as fluid is rest in a certain level and the air is filled rest of the domain.

Volume of fraction (VOF) is a multiphase flow model in Fluent. The VOF model can model two or more immiscible fluids by solving a single set of momentum equations and tracking the volume fraction of each of the fluids throughout the domain. The VOF model has been used in many CFD works for the pump (Bouziad *et al.* 2003, Bayeul-Lainé *et al.* 2012, Gruselle *et al.* 2011). The continuity equation of VOF model can be written as follows:

$$\frac{1}{\rho_q} \left(\frac{\partial}{\partial t} (\alpha_q \rho_q) + \nabla \cdot (\alpha_q \rho_q \vec{V}_q) \right) = S_{\alpha_q} + \sum_{p=1}^n (\dot{m}_{pq} - \dot{m}_{qp}) \quad (1)$$

If α_q equals to zero, the cell is empty (of the fluid). If α_q equals to one, he cell is full of the q^{th} fluid, $0 < \alpha_q < 1$ the cell contains the interface between the q^{th} fluid and one or more other fluids. Where \dot{m}_{pq} characterizes the mass transfer from phase q to phase p . S_{α_q} is mass source for each phase, ρ_q is the volume averaged density of the q^{th} phase in the solution domain, \vec{v}_q is the velocity of phase q and \dot{m}_{pq} characterizes the mass transfer from the p^{th} to q^{th} phase, and , and you are able to specify these mechanisms separately.

A single momentum equation is solved throughout the domain, and the resulting velocity field is shared among the phases. The momentum equation, shown

below, is dependent on the volume fractions of all phases through the properties ρ and μ .

$$\begin{aligned} \frac{\partial}{\partial t} (\rho \vec{V}) + \nabla \cdot (\rho \vec{V} \vec{V}) = \\ -\nabla P + \nabla [\mu (\nabla \vec{V} + \nabla \vec{v}^T)] + \rho \vec{g} + \vec{F} \end{aligned} \quad (2)$$

Where ρ is the volume-fraction-averaged density takes on the following form:

$$\rho = \sum \alpha_q \rho_q \quad (3)$$

k – ε Turbulence Model

The mixture turbulence model, which is used in the study, represents the first extension of the single-phase k-ε model, and it is applicable when phases separate, for stratified (or nearly stratified) multiphase flows, and when the density ratio between phases is close to 1. In these cases, using mixture properties and mixture velocities is sufficient to capture important features of the turbulent flow.

The k and ε equations describing this model are as follows:

$$\begin{aligned} \frac{\partial}{\partial t} (\rho_m k) + \nabla \cdot (\rho_m \vec{V}_m k) = \\ \nabla \cdot \left(\left(\mu_m + \frac{\mu_{t,m}}{\sigma_k} \right) \nabla k \right) + G_{k,m} - \rho_m \varepsilon \end{aligned} \quad (4)$$

$$\begin{aligned} \frac{\partial}{\partial t} (\rho_m \varepsilon) + \nabla \cdot (\rho_m \vec{V}_m \varepsilon) = \\ \nabla \cdot \left(\left(\mu_m + \frac{\mu_{t,m}}{\sigma_\varepsilon} \right) \nabla \varepsilon \right) + \frac{\varepsilon}{k} (C_{1\varepsilon} G_{k,m} - C_{2\varepsilon} \rho_m \varepsilon) \end{aligned} \quad (5)$$

where the mixture density, ρ_m , molecular viscosity, μ_m , and velocity, \vec{V}_m . The turbulent viscosity for the mixture, $\mu_{t,m}$, is computed from

$$\mu_{t,m} = \rho_m C_\mu \frac{k^2}{\varepsilon} \quad (6)$$

and the production of turbulence kinetic energy, $G_{k,m}$, is computed from

$$G_{k,m} = \mu_{t,m} \left(\nabla \vec{V}_m + (\nabla \vec{V}_m)^T \right) : \nabla \vec{V}_m \quad (7)$$

$C_{1\varepsilon}$, $C_{2\varepsilon}$, C_μ , σ_k and σ_ε are the model constants and these default values have been determined from experiments for fundamental turbulent flows.

Non-dimensional parameters

The non-dimensional parameters is useful when the new pump is based on an existing design. It is common to scale this design to produce a family of geometrically similar pumps which operate at different speeds. A key parameter that remains constant through such a scaling is the head coefficient. This is a measure of the energy transfer to the fluid and is defined as the head coefficient;

$$\psi = \frac{gH}{\omega^2 r^2} \quad (8)$$

where H is the head rise and r is the tip diameter. Similar to the head coefficient, the flow coefficient

remains the same for geometrically similar pumps. This is a measure of the flow rate through the pump and is defined as;

$$\phi = \frac{Q}{\omega r^2 b_2} \quad (9)$$

where Q is the impeller volume flow rate, ω is the rotational speed, and b_2 is tip width of the impeller.

2.3 Computational Grid

The mesh structure was generated by using ANSYS Meshing tool. The sweep meshes were used to shorten the simulation time and inflation layers were generated to model the near wall flow better. Two flow domain were created. One of them was a volume occurring by swept rotating the impeller and the other fixed remaining.

For mesh independence, three cases were identified in which the same analyzes were performed with different mesh densities. The analyzes were evaluated according to the flow coefficient of the pump. The number of elements in case 4 was determined as a reference according to the results in Table 1. Analyzes were performed with around the number of elements.

Table 1 The cases for mesh independence

Case	Number of Nodes	Total Elements	Flow coeff.
P1	153998	431794	0.03611
P2	195603	544178	0.03487
P3	284188	933546	0.03243
P4	345323	1189322	0.02483
P5	406146	1439181	0.02487

With reference to Case 5 given in Table 1, when the Eye Diameter, which is one of parameters in Table2, increased from 0.2 to 0.428, the total elements decreased from 1439181 to 1433972, showing a change of only 0.36%. Similarly, when the Stopper Length was reduced from 0.171 to 0, the total elements increased from 1439181 to 1448902, showing a change of only 0.67%. When analyzed in two other parameters, Expansion Rate and Upper Gap, the change in the total elements did not exceed 1%.

2.4 Optimization

An optimization study was carried out to obtain the optimal values of the four design parameters in accordance with the determined targets. Optimization studies were performed by using ANSYS Response Surface Optimization tool [Myers 1999, Yang and Xiao 2014] by setting the computational fluid dynamics (CFD) analysis to work. In Response Surface Optimization, a response surface is created by using the design points within the assigned range of the parameters. The best values for these parameters are determined according to the optimization method.

The values of the parameters were converted

dimensionless except the expansion rate since it is already dimensionless by proportioning the parameter values to the pump body diameter. Thus, a generalization can be made for a pump operating in the same manner using these ratios. The lower and upper values of the non-dimensional parameters in the optimization study are given in Table 2.

Table 2 The non-dimensional parameter limits for optimization of pump

Parameter	Lower Value	Upper Value
Eye Diameter	0.142	0.428
Expansion Rate	1.2	1.5
Stopper Length	0	0.171
Upper Gap	0.0214	0.0428

The most important problem will be the rise of the water in one of the lines above the limit values or the vacuum formation due to the penetration of air into the pump. If the rising of the water and the vacuum formation are considered as two different problems, they bring two limits which has to be avoid. The pump should neither from a vacuum inside its body nor let the fluid flow though both outlets at the same time. The water level should be identified and controlled as an output parameter and has to be added to the target values the analysis. Two output parameters were identified on the CFD at the outlet pipes and the hydrostatic pressure data on these levels were monitored. One of these levels was a plane which is 29 cm higher from the outlet of the pump, can be considered a steady rising point to read the pressure more smoothly. Also, a plane 2 cm higher from the outlet pump was defined since the water level can fall below 2 cm when vacuum is formed (Fig. 2). Since these planes were not on which the push line of the pump, on the other line, it is aimed to minimize the head coefficients on these planes.

In the simulation the discharge line is 69 cm higher from the pump outlet and it is making a u-turn all the way through beginning position. While the pump is working to the discharge line, a low pressure occurs inside the elbow which yields the more flow rate than which pump carries out. But result of that it is seen vacuum formation in the recirculation line.

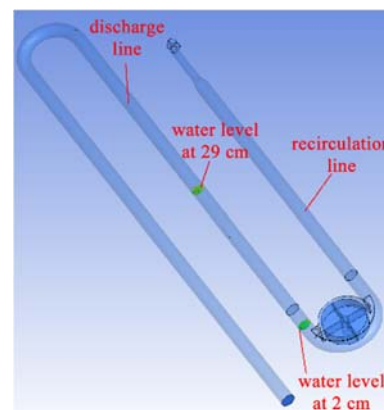


Fig. 2. Specified surface to monitor the water level

The target value was set to minimize the pressure on the plane and to maximize the flow rate at the operating outlet. Optimum pump geometry values obtained as a result of the optimization shown in Table 3. This pump is shown in Fig. 3. The simulation results of the which operating in the recirculation line and discharge line can be seen in Table 4 and Table 5, respectively.

Table 3 Non-dimensional parameter values of the optimal pump

Parameter	Value
Eye Diameter	0.322
Expansion Rate	1.2
Stopper Length	0.1028
Upper Gap	0.022

The optimization result show that, the eye diameter was found to be closer to the upper value by 0.322. The reason is that in the bigger diameter values, the flow coefficient is higher than the other line. The optimal value of the expansion rate was the lowest value because of increase of the pressure in the other line, it is attached to the optimization constraint. Similarly, bigger values of the stopper length and upper gap causes the pressure increase in the other line.

While the pump is operating through to the recirculation line, it appears that there is an increase of the water level 56 cm from the pump on the discharge line and a 48 cm rise on the recirculation line while operating though the discharge line. However, since these values are obtained as the result of the optimization, they should be considered as the smallest which can be obtained within the limits. The desired flow coefficient for recirculation and discharge were achieved. In Fig. 4 can be seen air volume fraction when the pump pushes to recirculation line, water doesn't exceed the u-turn as expected. In Fig. 5 can

be seen air volume fraction when the pump pushes to discharge line, a vacuum doesn't occur in the pump. Velocity vectors and eddy viscosity contours can be seen in Fig. 6 when the pump works to discharge line (clockwise).

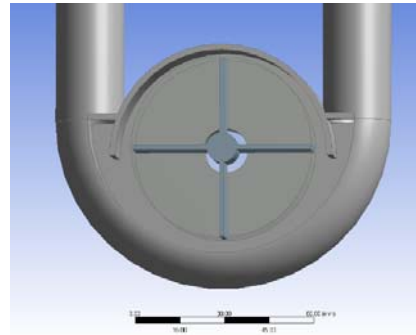


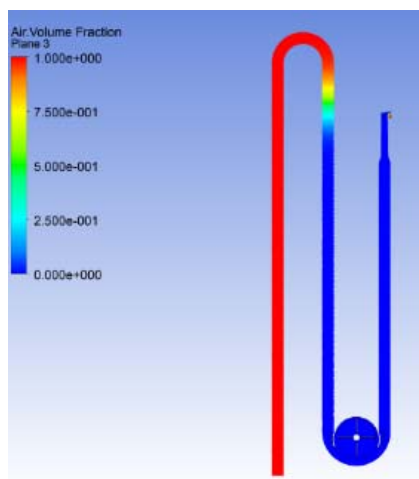
Fig. 3. Optimum pump geometry

Table 4 Simulation results operating in the recirculation line

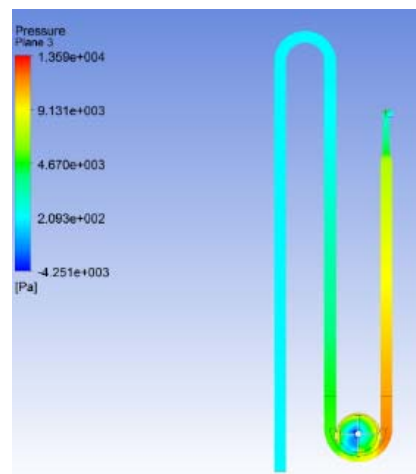
Output Parameter	Value
Flow coefficient	0.02016
Efficiency	%18.76
Head at 2 cm	56 cm
Head at 29 cm	29 cm

Table 5 Simulation results operating in the discharge line

Output Parameter	Value
Flow coefficient	0.0358
Efficiency	%19.47
Head at 2 cm	48 cm
Head at 29 cm	22 cm



a)



b)

Fig. 4. When operated in the recirculation line, a) the volume fraction contours, b) the pressure contours

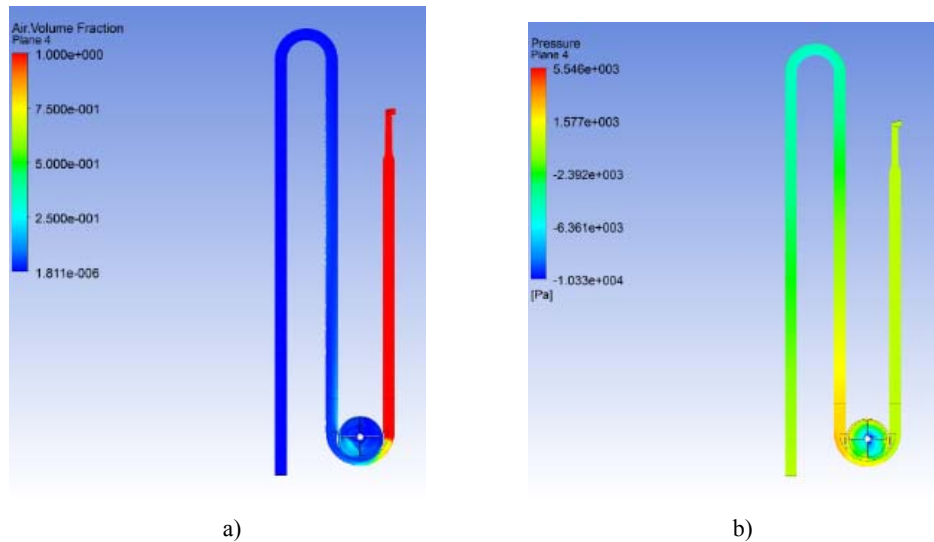


Fig. 5. When operated in the discharge line, a) the volume fraction contours, b) the pressure contours

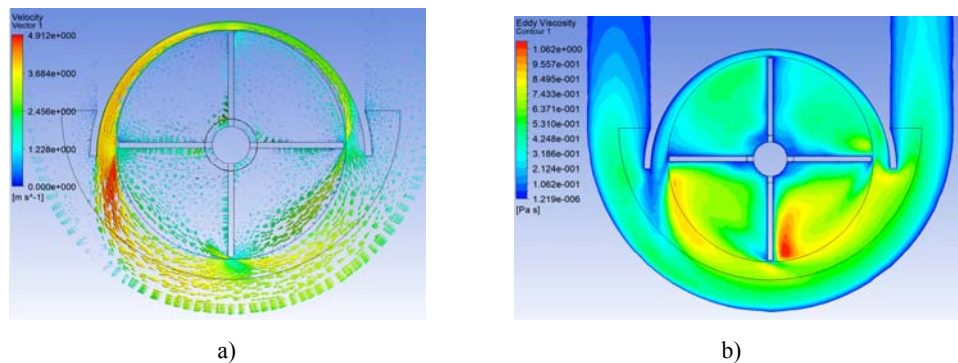


Fig. 6. a) Velocity vectors b) Eddy viscosity contours

2.5 Parametric relationships

Relations between input parameters such as expansion rate, eye diameter, stopper length, upper gap and output parameters such as recirculation flow rate, water levels, efficiency were revealed with CFD analysis, can be seen in Fig. 7. According to these results, the head coefficient in the discharge line and efficiency values don't change after about 0.2 of eye diameter. After about 0.35 of eye diameter, the value of the flow coefficient decreases slightly. While the increasing value of the expansion rate leads to a low linear increase in the flow coefficient, the increase acceleration of the head coefficient in the discharge line and efficiency decreases after about 1.3. While the stopper length has no effect on the flow coefficient as can be expected, it has a low effect with increasing value on the head coefficient in the discharge line and efficiency. The increase in the value of the upper gap is an increase for all.

3. EXPERIMENTAL STUDY

To validate the numerical results it is necessary to build a test set-up and create the similar physical condition. To realize that a water tank was manufactured with a discharge pipe at the bottom of the tank which connected to the pump and two outlets connected from the pump to the tank.

Krohne OptiBar 1010C pressure transmitters, which produce a signal current of 4-20mA and measure the range of 0-250 mbar, were used to measure the pressure at the inlet and outlets of the pump. IFM SM7100 flow meter which produces a signal current of 4-20 mA and measure between 0-50 l/min was used to measure the flow rate. To measure the flow rate the flow meter was connected to the suction line before the pressure transmitter. A torque sensor, Kistler 4205A6HA, was also placed to measure the consumed power and a controllable motor was connected to the impeller to adjust the rotation speed. The NI cDAQ 9178 8-slot USB chassis was used as a data acquisition device. Signals sent from pressure transmitter and flow meter were received with the NI 9203 module. The NI 9215 was used to received the signal of the torque sensor because it is being used to convert voltage signals. The NI 9263 is an output module which was used to drive the electric motor. Labview Signal Express software was used to collect the data. Whole test set-up and schematic test setup of water and electrical line can be seen in Figs. 8 and 9, respectively.

Pump head (H) can be calculated as follows;

$$H = \frac{P_d - P_s}{\rho g} + (z_d - z_s) \quad (10)$$

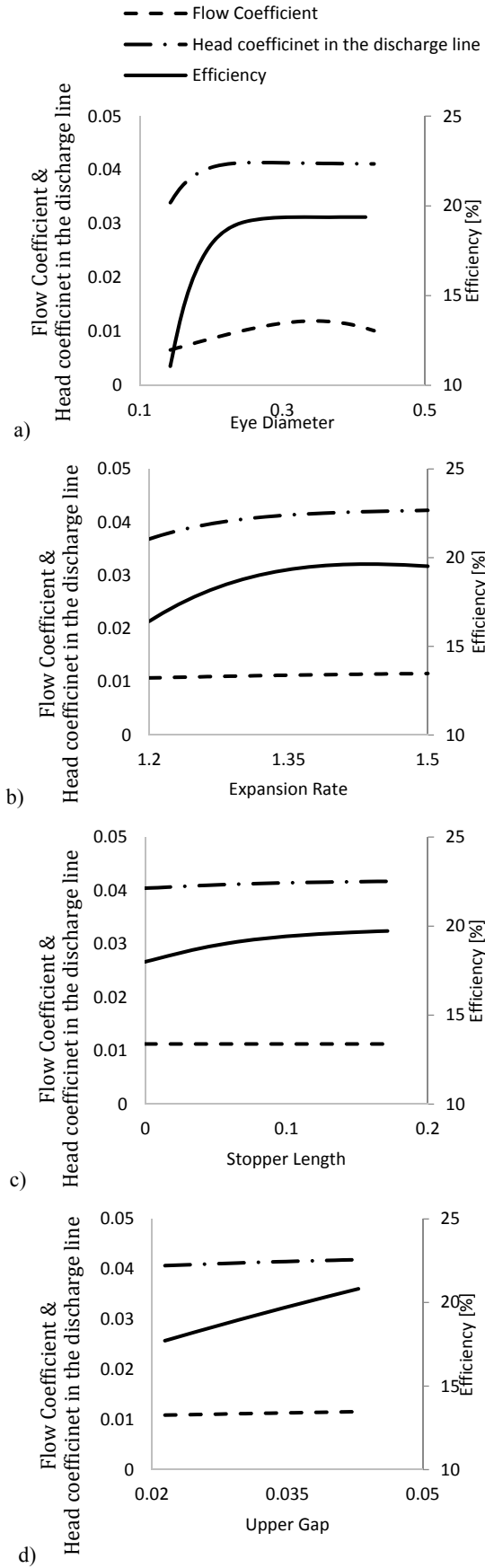


Fig. 7. Dependence of output parameters on non-dimensional a) eye diameter, b) expansion rate, c) stopper length, d) upper gap

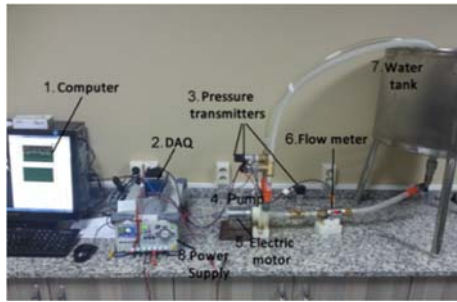


Fig. 8. The test setup

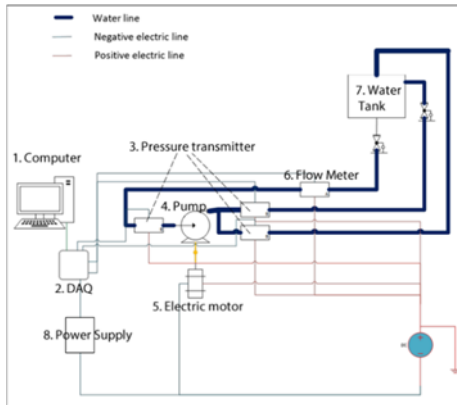


Fig. 9. Schematic test setup of water and electrical line

where P_d is discharge pressure, P_e is suction pressure, $(z_d - z_s)$ is the distance between discharge and suction. The velocity was neglected since suction and discharge diameters of the pump are approximately the same in size. Pump efficiency can be expressed as;

$$\eta = \frac{\rho g Q H}{\dot{W}_{shaft}} \quad (11)$$

$$\dot{W}_{shaft} = I \cdot V \cdot \eta_{motor} \quad (12)$$

3.1 Test Results

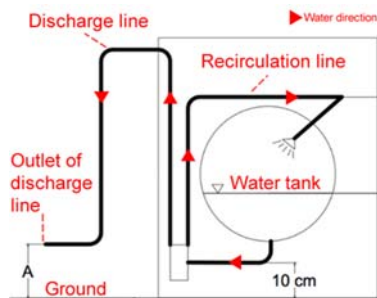


Fig. 10. Fixed dimensions of the measurement

The pump was placed 10 cm above the ground. The height at which outlet of the water exists is indicated as (A). While pump is pushing the discharge line, If the vacuum occurs in the test, the height of (A) was increased and it was determined by means of the height the level of start where the vacuum is formed (Fig. 10), because the bigger values of (A) prevents vacuum formation in recirculation line. Different pumps were

manufacture depending on the CFD analyzes and experimental knowledge about the pump. The labels were designated based on the specific characteristics of the pumps so that the pumps to track the test results more easily (Fig. 11).

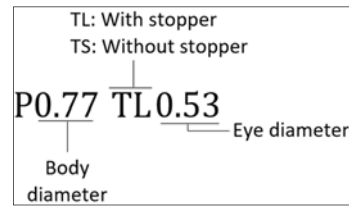


Fig. 11. The pump labels

The non-dimensional body diameters are a ratio to maximum diameter of the study. Similarly, the dimensionless speed values are the ratio to 3300 rev/min, the maximum speed of the study. The test results can be seen in the Table 6.

- The P0.77TL0.142 and the P1TL0.142 cannot pump the water to the discharge line due to the small inlet cross-section, and the recirculation valve seems to be insufficient.
- The P0.77TL0.2 and P0.77TL0.228 are provided desired flow rate. Water heights of the recirculation line and discharge line are obtained as 48 cm and 50 cm, respectively. However, when the P0.77TL0.2 operates through the discharge line if exit of the line is lower than 15 cm from the ground, the vacuum occurs in the recirculation line. The same situation occurs below the 5 cm height for the P0.77TL0.228. It is more convenient to use the P0.77TL0.228 if this vacuum is considered.
- The P0.88TL0.214 and the P0.88TS0.214 also provide desired flow rates and the water rise in the discharge line acceptable in the recirculation operation. If the exit of the discharge line is kept below the given vacuum values, vacuum is beginning to appear in the recirculation lines of the pumps.
- Pumps with different specifications with body diameter of 1 were tested. P1TS0.2 starts to form vacuum at exit distances of less than 10 cm from the ground. All other pumps of body diameter of 1 are in acceptable flow rate and water level values.
- In pumps tested at the same body diameter and at the same speed, the increased eye diameter provides an improvement in flow coefficient, while the starting point of vacuum formation is also reduced. (P0.77TL0.2, P0.77TL0.228).
- When the pumps with stopper or without stopper tested at the same body diameter, eye diameter and speed are examined, the flow coefficient decreases slightly in with the stopper pump while the increase in the recirculation line is somewhat reduced, at the same time, as a positive result is that the vacuum formation starts at a lower level in the stopper pump (P0.88TL0.214, P0.88TS0.214).

Table 6 Test results

Pump label	Speed (..)	Flow coefficient of resirculation line (...)	Flow coefficient of discharge line (..)	Water height in the recirculation line (cm)	(A) height of the starting of vacuum formation point (cm)
P0.77TL0.142	0.838	0.00693	0	at limit	40
P0.77TL0.2	0.515	0.01319	0.02485	48 cm	15
P0.77TL0.228	0.515	0.01376	0.02772	50 cm	5
P0.88TL0.214	0.454	0.01493	0.02405	53	20
P0.88TS0.214	0.454	0.01443	0.02372	50	10
P1TL0.142	0.454	0.00550	0	37	30
P1TL0.2	0.454	0.01297	0.01913	51	-
P1TL0.214	0.454	0.01402	0.02005	59	-
P1TL0.228	0.418	0.01353	0.02464	55	-
P1TL0.228	0.435	0.01466	0.02548	60	-
P1TS0.2	0.454	0.01297	0.01900	51	10
P1TS0.214	0.454	0.01376	0.01966	58	-
P1TS0.228	0.454	0.01415	0.02228	58	-

- Increasing body diameter minimizes the starting point of vacuum formation. While the increasing eye diameter increases the flow coefficient, water height in the recirculation line also increases (P1TL0.2, P1TL0.214).
- The increased speed increases the flow coefficient but also increases the water height on the other side (P1TL0.228 at 0.418 of speed, P1TL0.228 at 0.435 of speed).
- With the eye diameter increasing in stopper pumps, the A level decreases even goes down to 0 (P1TS0.2, P1TS0.214, P1TS0.228).

3.2 Pump Performance Curves by CFD and Experimental

The test and simulation results of the pumps were compared by head coefficient-flow coefficient-efficiency curves. Firstly, according to these results, there was a good agreement between CFD results and test results. While the best efficiency value is obtained with the P1TL0.214 and P0.88TL0.214 pumps, when the 0.01 value of the flow coefficient is taken as reference. the maximum head coefficient at this point is again obtained in the P0.88TL0.214 pump. When the same flow coefficient reference is taken, head coefficient and efficiency increase with increasing eye diameter in the pumps with the same body diameter. The maximum head coefficient are observed in P1TL0.2, P0.88TS0.214 and P1TS0.2, respectively, but the highest efficiency points are lower than the other pumps. Separately, the head coefficient at 0.01 flow coefficient are well below these points, because the losses are increasing in these pumps with increased flow coefficient. Except these three pumps, there is no significant

difference of the head coefficient values at which between the 0.01 flow coefficient and maximum efficiency point, because the losses are relatively less with increasing flow coefficient in other pumps.

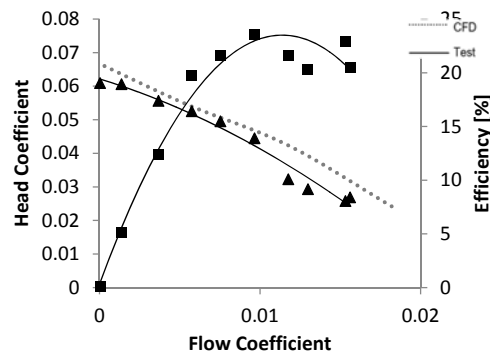


Fig. 12. The comparison of P1TL0.2

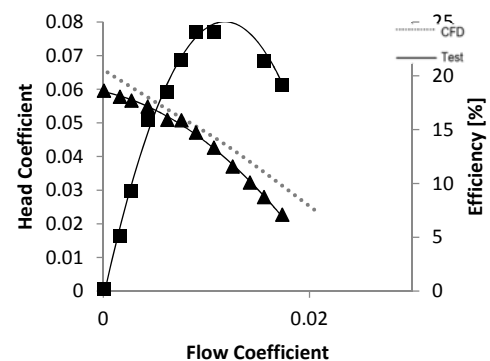


Fig. 13. Comparison of P1TL0.214

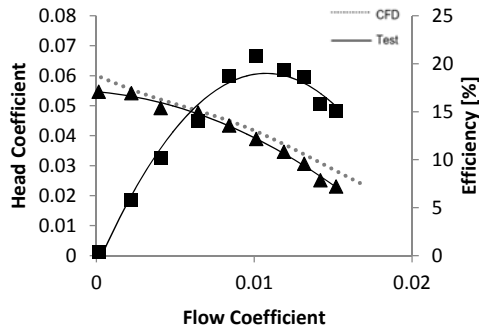


Fig. 14. Comparison of P1TS0.2

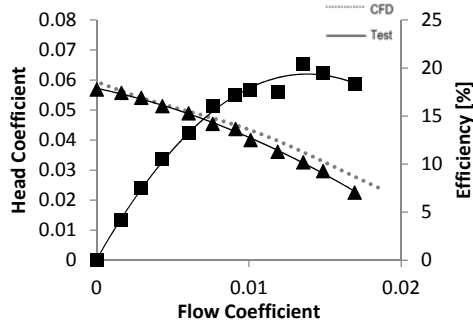


Fig. 15. Comparison of P1TS0.214

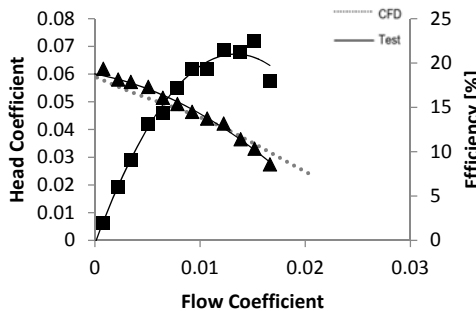


Fig. 16. Comparison of P1TS0.228

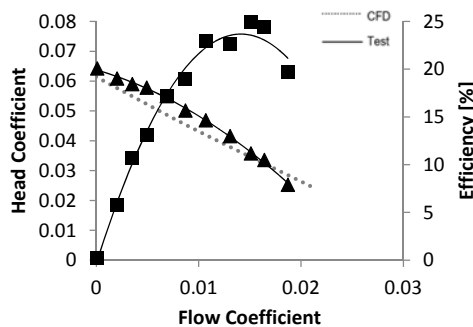


Fig. 17. Comparison of P0.88TL0.214

4 CONCLUSION

In this study, a single suction double outlet pump design was realized. For this purpose, the volute casing was designed with two exit lines, which are in the same directions. The impeller of the pump has flat blades to pump the fluid through each line.

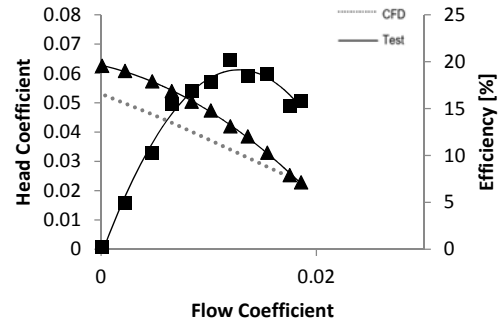


Fig. 18. Comparison of P0.88TS0.214

according to the direction of rotation. Both outlets were designed to have the same volute effect with the rotation. In these conditions, the geometric parameters which can affect the pump performance were determined. Optimal pump design was searched by performing a parametric optimization study with ANSYS Response Surface using the data by CFD calculations. In the optimization study, it is investigated that if the desired flow rate and pump head is according to the direction of rotation of the impeller. While the pump operates through one line, the situation in the other line is also monitored. The some pump designs are manufactured and tested to ensure that if they can provide the desired conditions. Finally CFD results and experimental results were compared. Obtained results proved that P1TL0.2, P1TL0.214, P1TL0.228, P1TS0.214 and P1TS0.228 pumps can provide the satisfied conditions. It was seen that the effect of the stoppers is not very important. The small suction eye diameter is unable to perform a proper pump operation. The height of the starting of vacuum formation point (A) has very important effect on the performance of the pump especially on vacuum formation and it should not be lower than 5 cm below the inlet level of the pump.

ACKNOWLEDGMENT

The authors gratefully acknowledge TUBITAK for making this project possible under TEYDEB 1505 Grant No. 5130031.

REFERENCES

- Asuaje, M., Bakir, F., Koudri, S., Kenyery, F., & Rey, R. (2005). Numerical modelization of the flow in centrifugal pump: volute influence in velocity and pressure fields. *International journal of rotating machinery* 2005(3), 244-255.
- Barrio, R., Parrondo, J., & Blanco, E. (2010). Numerical analysis of the unsteady flow in the near-tongue region in a volute-type centrifugal pump for different operating points. *Computers & Fluids* 39(5), 859-870.
- Bayeul-Lainé, A. C., Simonet, S., Bois, G., & Issa, A. (2012). Two-phase numerical study of the flow field formed in water pump sump: influence of air entrainment. In *IOP*

- Conference Series: Earth and Environmental Science* (Vol. 15, No. 2, p. 022007). IOP Publishing.
- Bouziad, Y. A., Farhat, M., Guennoun, F., Kueny, J. L., Avellan, F., & Miyagawa, K. (2003, November). Physical Modelling and Simulation of Leading Edge Cavitation-Application to an Industrial Inducer. In *Proceedings of the 5th International Symposium on Cavitation (CAV2003)* (pp. 1-4), Osaka, Japan.
- Chalghoum, I., Elaoud, S., Akrouf, M., & Taieb, E. H. (2016). Transient behavior of a centrifugal pump during starting period. *Applied Acoustics* 109, 82-89.
- Cooper, P., Tchobanoglous, G., Garbus, R. O., Hart, R. J., Reh, C. W., Sloan, L. G., & Smith, E. C. (2008). *Performance of centrifugal pumps*. In *Pumping Station Design* (Third Edition) (pp. 10-1).
- Damor, J. J., Patel, D. S., Thakkar, K. H., & Brahmabhatt, P. K. (2013). Experimental and CFD Analysis Of Centrifugal Pump Impeller-A Case Study. *International Journal of Engineering Research & Technology*.
- Dick, E., Vierendeels, J., Serbrugyns, A., & Voorde, J. V. (2001). Performance prediction of centrifugal pumps with CFD-tools. *Task quarterly* 5, 579-594.
- Dixon, S. L., & Hall, C. (2010). *Fluid mechanics and thermodynamics of turbomachinery*. Butterworth-Heinemann, Oxford, UK.
- Douglas, P. W. (1964). *U.S. Patent No. 3,136,254*. Washington, DC: U.S. Patent and Trademark Office.
- Francois, T. P. (1959). *U.S. Patent No. 2,916,997*. Washington, DC: U.S. Patent and Trademark Office.
- Grapsas, V., Stamatelos, F., Anagnostopoulos, J., & Papanonis, D. (2008, September). Numerical study and optimal blade design of a centrifugal pump by evolutionary algorithms. In *International Conference on Knowledge-Based and Intelligent Information and Engineering Systems* (pp. 26-33). Springer, Berlin, Heidelberg.
- Gruselle, F., Steimes, J., & Hendrick, P. (2011). Study of a two-phase flow pump and separator system. *Journal of engineering for gas turbines and power* 133(6), 062401.
- Jafarzadeh, B., Hajari, A., Alishahi, M. M., & Akbari, M. H. (2011). The flow simulation of a low-specific-speed high-speed centrifugal pump. *Applied Mathematical Modelling* 35(1), 242-249.
- Ling, Z., Weidong, S., Weigang, L., Rongjun, X., & Chuan, W. (2011). Orthogonal test and optimization design of submersible pump guide vanes. *Journal of Drainage and Irrigation Machinery Engineering* 29(4), 312-315.
- Munson, B. R., Okiishi, T. H., Rothmayer, A. P., & Huebsch, W. W. (2012). *Fundamentals of fluid mechanics*. John Wiley & Sons, NJ, USA.
- Myers, R. H. (1999). Response surface methodology--current status and future directions. *Journal of Quality Technology* 31(1), 30.
- Olszewski, P. (2016). Genetic optimization and experimental verification of complex parallel pumping station with centrifugal pumps. *Applied Energy* 178, 527-539.
- Park, S. K. (2012). *U.S. Patent No. 8,122,547*. Washington, DC: U.S. Patent and Trademark Office.
- Petit, O., Page, M., Beaudoin, M., & Nilsson, H. (2009, October). The ERCOFTAC centrifugal pump OpenFOAM case-study. In *Proceedings of the 3rd IAHR International Meeting of the Workgroup on Cavitation and Dynamic Problem in Hydraulic Machinery and Systems*, Brno, Czech Republic.
- Shah, S. R., Jain, S. V., & Lakhera, V. J. (2010, December). CFD based flow analysis of centrifugal pump. In *Proceedings of the 37th National & 4th International Conference on Fluid Mechanics and Fluid Power*, IIT Madras, Chennai.
- Shah, S. R., Jain, S. V., Patel, R. N., & Lakhera, V. J. (2013). CFD for centrifugal pumps: a review of the state-of-the-art. *Procedia Engineering* 51, 715-720.
- Singh, R. R., & Nataraj, M. (2012). Optimizing impeller geometry for performance enhancement of a centrifugal blower using the taguchi quality concept. *International Journal of Engineering Science and Technology* 4(10).
- Spence, R., & Amaral-Teixeira, J. (2009). A CFD parametric study of geometrical variations on the pressure pulsations and performance characteristics of a centrifugal pump. *Computers & Fluids* 38(6), 1243-1257.
- Yang, W., & Xiao, R. (2014). Multiobjective optimization design of a pump-turbine impeller based on an inverse design using a combination optimization strategy. *Journal of Fluids Engineering* 136(1), 014501.
- Zhang, Y., Hu, S., Wu, J., Zhang, Y., & Chen, L. (2014). Multi-objective optimization of double suction centrifugal pump using Kriging metamodels. *Advances in Engineering Software* 74, 16-26.
- Zhou, W., Zhao, Z., Lee, T. S., & Winoto, S. H. (2003). Investigation of flow through centrifugal pump impellers using computational fluid dynamics. *International Journal of Rotating Machinery* 9(1), 49-61.